Supplementary Data

A novel photocatalytic carbon dots: efficiently inhibiting amyloid aggregation and quickly disaggregating amyloid aggregates

Xu Shao [a], Chao Wang [a], Chaoli Wang [b] Mengyao Bai [a], Tongtong Hou [a], Xin Wang [a], Chaoren Yan [c], Ping Guan [a*], Xiaoling Hu [a*]*

[a] Department of Chemistry, School of Chemistry and Chemical Engineering, Northwestern Polytechnical University, 127 Youyi Road, Xi'an 710072, China

[b] Department of Pharmaceutical Chemistry and Analysis, School of Pharmacy, Air Force Medical University, 169 Changle West Road, Xi'an 710032, China

[c] School of Medicine, Xizang Minzu University, Key Laboratory for Molecular Genetic Mechanisms and Intervention Research on High Altitude Disease of Tibet Autonomous Region, Xianyang, Shaanxi 712082, China

E-mail: yanchaoren@mail.nwpu.edu.cn (Chaoren Yan)

E-mail: guanping1113@nwpu.edu.cn (Ping Guan)

E-mail: huxl@nwpu.edu.cn (Xiaoling Hu)

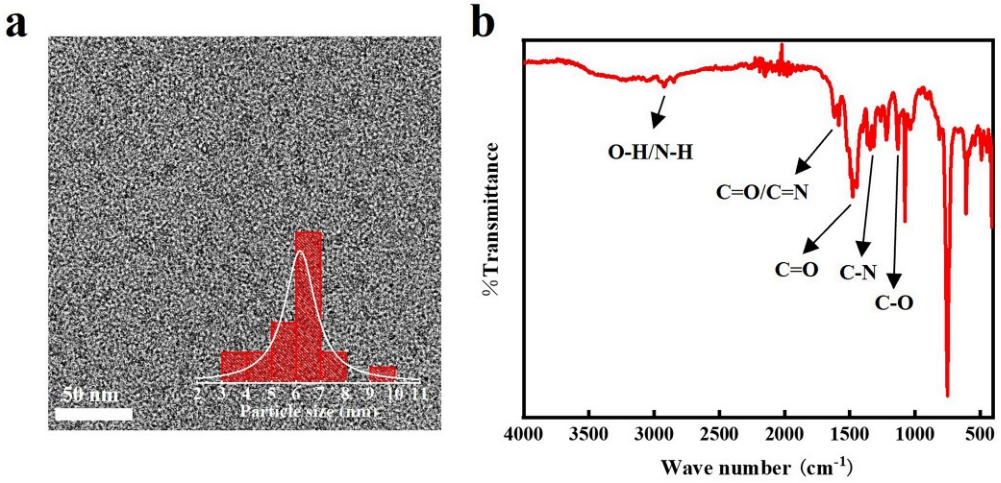

Figure S1. (a) TEM image of CNDs after irradiation. (b) FTIR spectrum of CNDs after irradiation.

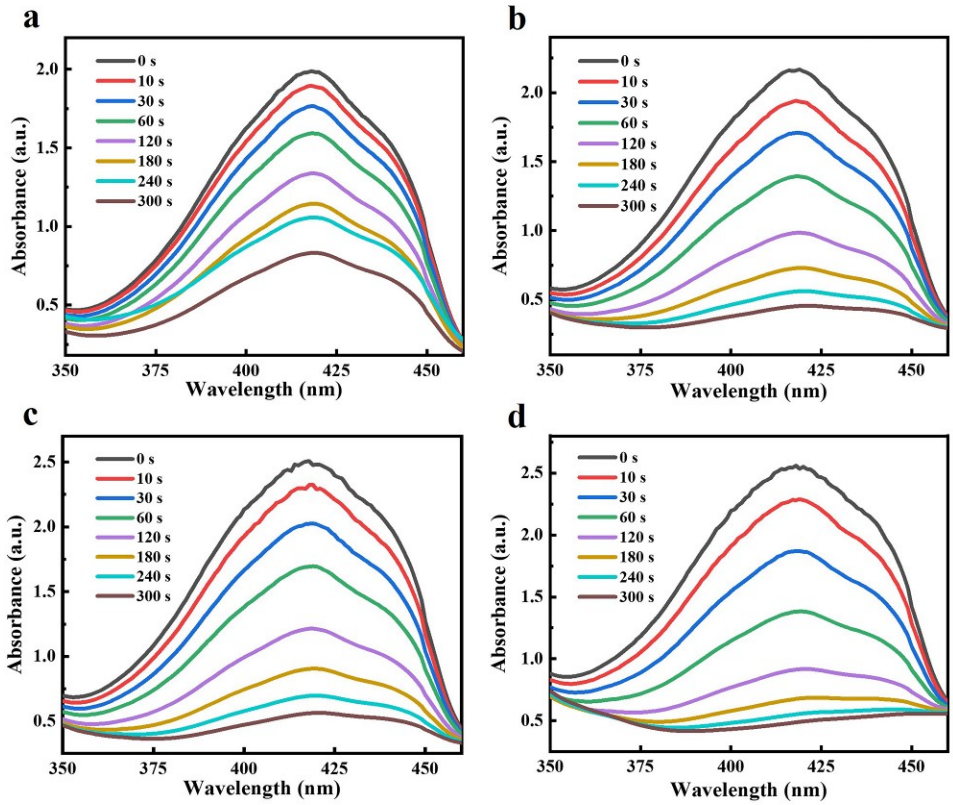

Figure S2. DPBF was used to detect the generation of singlet oxygen of CNDs with different concentrations under 580 nm irradiation. (a) 3 μg/mL (b) 6 μg/mL (c) 12 μg/mL and (d) 24 μg/mL.

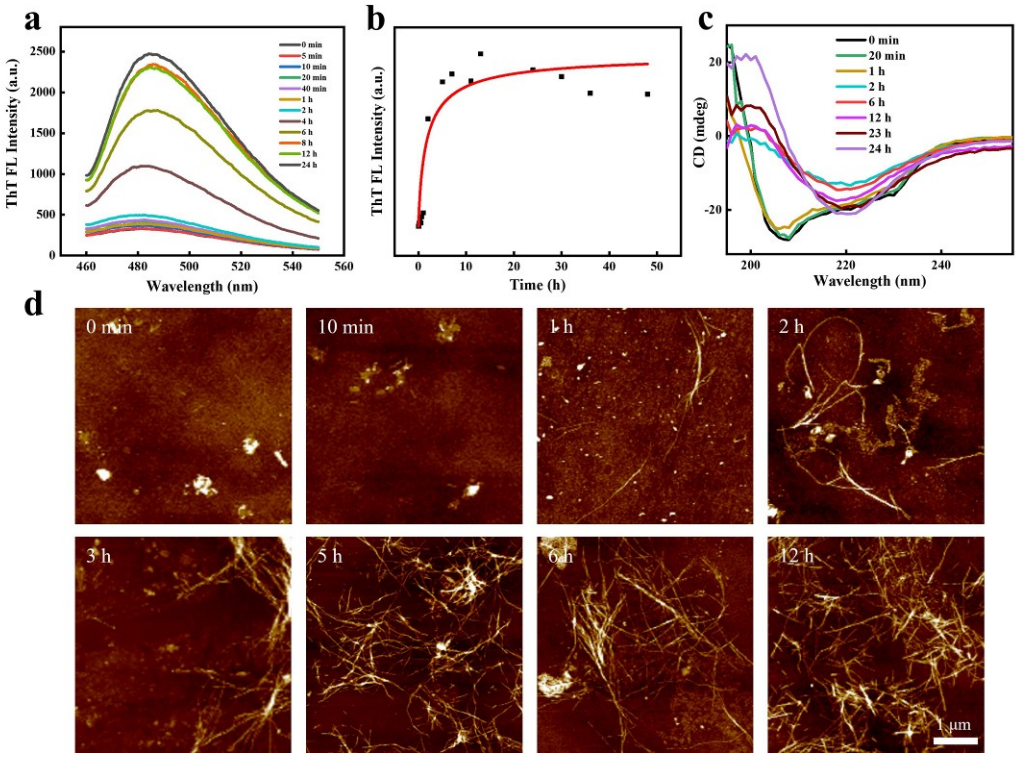

Figure S3. Lysozyme fibrosis process. (a-b) ThT fluorescence assay to quantify the aggregation of lysozyme. (c) CD spectrum of lysozyme incubated for 24 h. (d) AFM images of lysozyme fibrils samples cultured at various time.

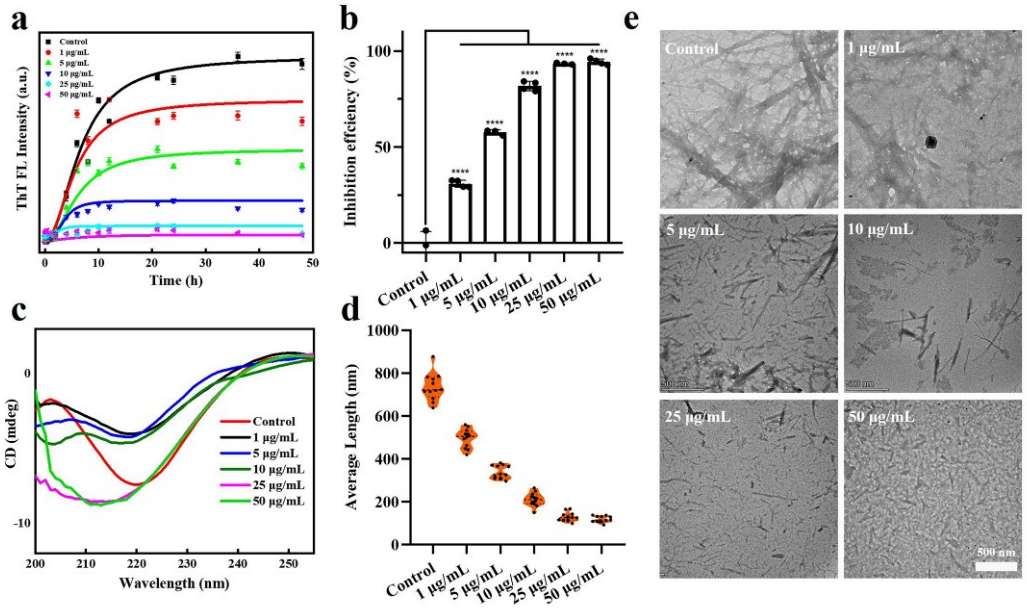

Figure S4. Inhibition of the lysozyme fibrillation process by CNDs. (a) ThT kinetic aggregation profiles to quantify the inhibition of lysozyme in the presence of CNDs at different concentrations. (b) The corresponding inhibition efficiencies of CNDs for lysozyme fibrillation. (c) CD spectra of lysozyme in the presence of CNDs at different concentrations after 48h incubation. (d) The corresponding size distribution of TEM results, dashed lines represent medians. (e) TEM images of lysozyme co-incubated in the presence of different concentration CNDs for 48 h. (****, $p < 0.0001$).

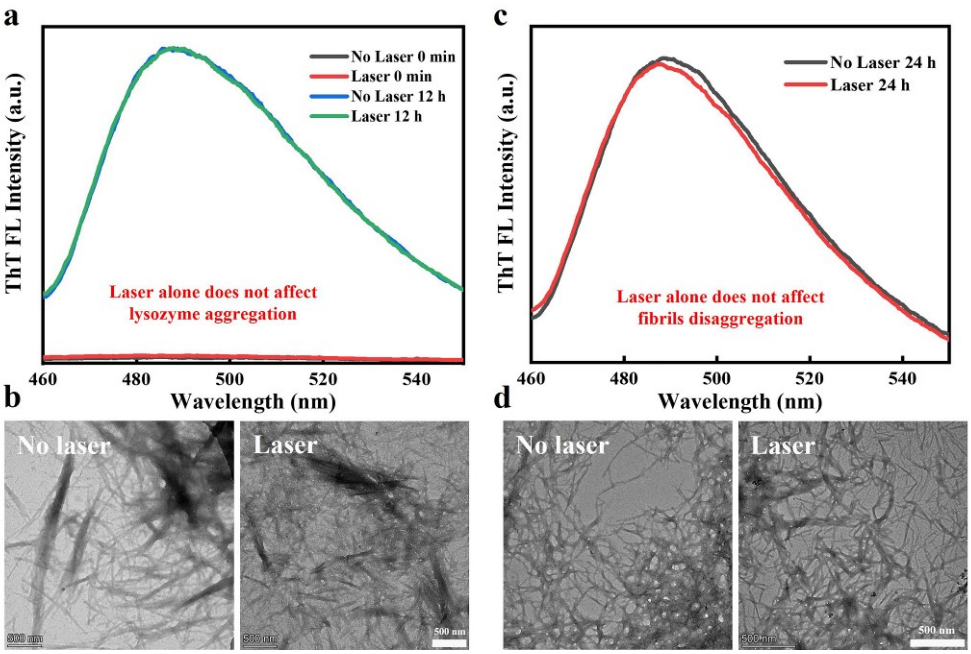

Figure S5. Effects of laser alone on lysozyme aggregation and disaggregation. (a) ThT fluorescence to quantify the fibrosis of lysozyme with laser alone. (b) TEM images of lysozyme. (c) ThT fluorescence to quantify the disaggregation of lysozyme with laser alone. (d) TEM images of lysozyme aggregates.

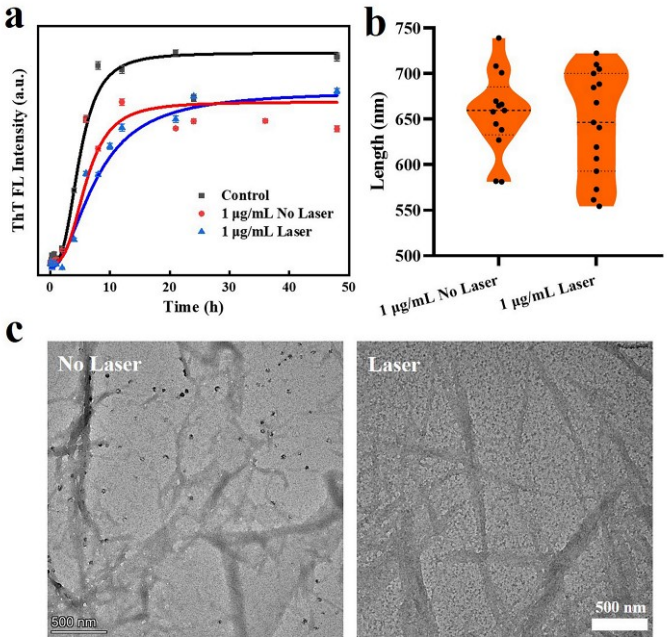

Figure S6. Inhibition effect of 1 μg/mL CNDs on lysozyme. (a) ThT kinetic aggregation profiles to quantify the inhibition of lysozyme in the presence of CNDs at 1 μg/mL. (b) The corresponding size distribution of TEM results, dashed lines represent medians. (c) TEM images of lysozyme co-incubated in the presence of 1 μg/mL CNDs for 48 h.

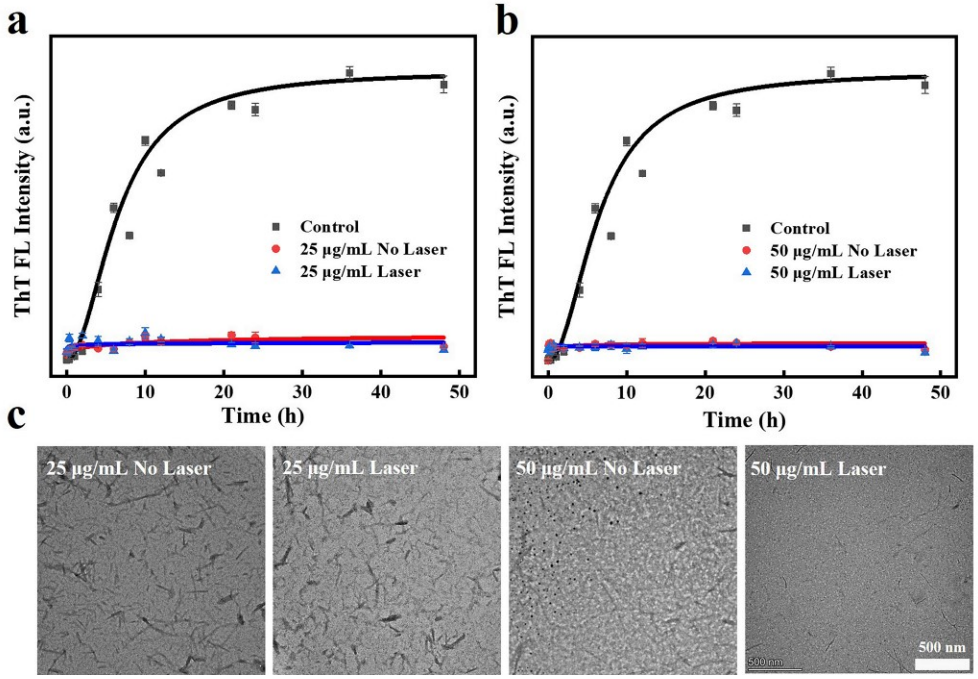

Figure S7. Inhibition effect of high concentration CNDs on lysozyme. (a) ThT kinetic aggregation profiles to quantify the inhibition of lysozyme in the presence of CNDs at 25 μg/mL. (b) ThT kinetic aggregation profiles to quantify the inhibition of lysozyme in the presence of CNDs at 50 μg/mL. (c) TEM images of lysozyme co-incubated in the presence of 25 μg/mL or 50 μg/mL CNDs for 48 h.

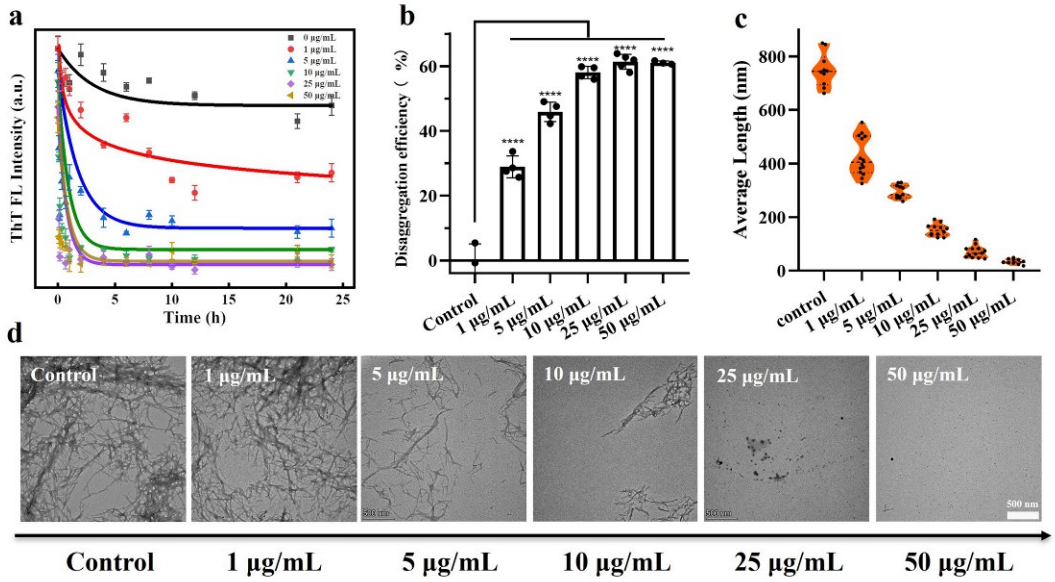

Figure S8. Disaggregation of the lysozyme aggregates by CNDs without irradiation. (a) ThT kinetic aggregation profiles to quantify the disaggregation of lysozyme in the presence of CNDs at different concentrations. (b) The corresponding disaggregation efficiencies of CNDs. (c) The corresponding size distribution of TEM results, dashed lines represent medians. (d) TEM images of lysozyme aggregates co-incubated in the presence of different concentration CNDs for 48 h. (****, $p < 0.0001$).

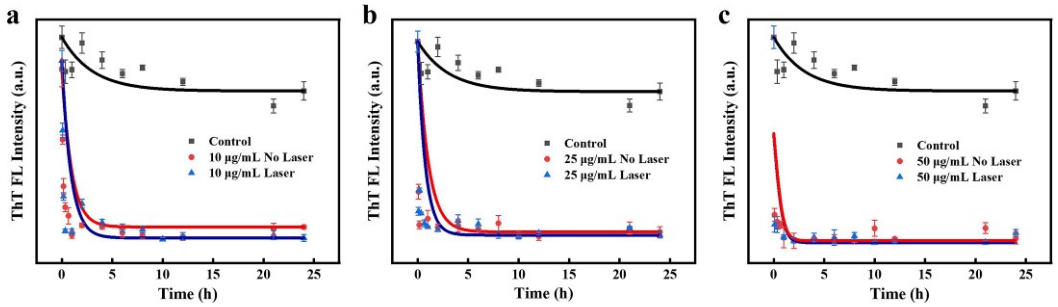

Figure S9. Disaggregation effect of high concentration CNDs. (a) 10 μg/mL (b) 25 μg/mL and (c) 50 μg/mL CNDs co-incubated with 1.25 mg/mL lysozyme aggregates.

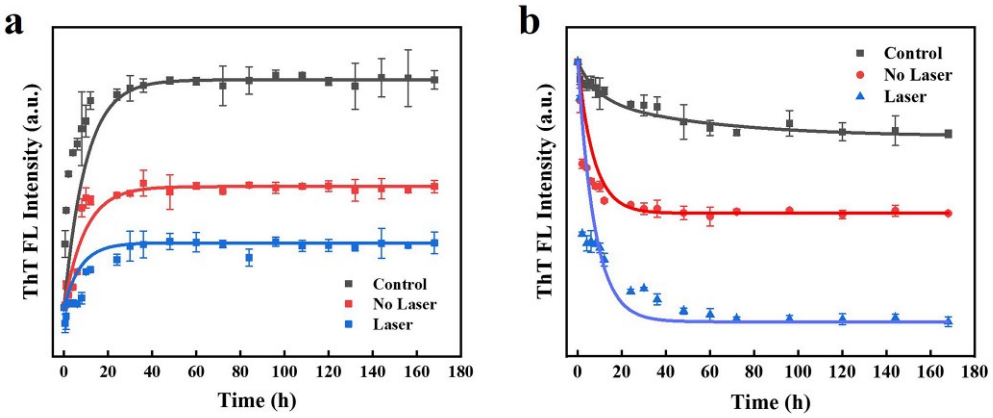

Figure S10. Long-term inhibition of Aβ42 aggregation and acceleration of Aβ42 aggregate disaggregation by 10 μg/mL CNDs.